

Pharmacological Rescue of the Mutant Cystic Fibrosis Transmembrane Conductance Regulator (CFTR) Detected by Use of a Novel Fluorescence Platform

John P Holleran,^{1,2} Matthew L Glover,¹ Kathryn W Peters,¹ Carol A Bertrand,¹ Simon C Watkins,¹ Jonathan W Jarvik,² and Raymond A Frizzell¹

¹Department of Cell Biology, University of Pittsburgh School of Medicine, Pittsburgh, Pennsylvania, United States of America; and

²Department of Biological Sciences, Carnegie Mellon University, Pittsburgh, Pennsylvania, United States of America

Numerous human diseases arise because of defects in protein folding, leading to their degradation in the endoplasmic reticulum. Among them is cystic fibrosis (CF), caused by mutations in the gene encoding the CF transmembrane conductance regulator (CFTR), an epithelial anion channel. The most common mutation, F508del, disrupts CFTR folding, which blocks its trafficking to the plasma membrane. We developed a fluorescence detection platform using fluorogen-activating proteins (FAPs) to directly detect FAP-CFTR trafficking to the cell surface using a cell-impermeant probe. By using this approach, we determined the efficacy of new corrector compounds, both alone and in combination, to rescue F508del-CFTR to the plasma membrane. Combinations of correctors produced additive or synergistic effects, improving the density of mutant CFTR at the cell surface up to ninefold over a single-compound treatment. The results correlated closely with assays of stimulated anion transport performed in polarized human bronchial epithelia that endogenously express F508del-CFTR. These findings indicate that the FAP-tagged constructs faithfully report mutant CFTR correction activity and that this approach should be useful as a screening assay in diseases that impair protein trafficking to the cell surface.

Online address: <http://www.molmed.org>

doi: 10.2119/molmed.2012.00001

INTRODUCTION

Cystic fibrosis (CF), the most common lethal genetic disease among Caucasians, is caused by mutations in the CF transmembrane conductance regulator (CFTR) gene (1). CFTR is an anion channel that is responsible for adenosine 3',5'-cyclic monophosphate (cAMP)/cAMP-dependent protein kinase (PKA)-stimulated secretion of chloride and bicarbonate ions across the apical membranes of polarized epithelial cells (2). CFTR is a type II transmembrane protein consisting of two membrane-spanning domains, each composed of six membrane-spanning α -he-

lices, two cytoplasmic nucleotide binding domains (NBD) and a central cytoplasmic regulatory domain, the predominant site of PKA phosphorylation (3). Although there are many documented mutations in CFTR, by far the most prevalent mutation, the deletion of F508 in NBD1 (F508del) is present on at least one allele in 90% of CF patients (4). This mutation causes protein misfolding that results in premature proteasomal degradation, and it precludes channel expression at the cell surface (5,6). The trafficking of F508del-CFTR to the plasma membrane can be partially rescued, however, by

low temperature (<30°C) or with chemical chaperones such as glycerol (6–8).

Recent efforts are aimed at the discovery of small molecules that remedy the folding of mutant CFTR and promote its trafficking to the plasma membrane. High-throughput drug screening efforts have successfully identified many small molecule compounds that partially rescue the trafficking defect of F508del-CFTR, called correctors (9–12). Thus far, correctors have shown limited ability to improve F508del-CFTR trafficking. Even after corrector treatment, F508del-CFTR has <15% the activity of CFTR wild-type (WT), and the corrector efficacy may vary depending on the cell type examined (13–16). More robust rescue can be achieved by using a combination of correctors, which enhances rescue to levels greater than individual compound actions (17–19).

To date, most F508del-CFTR corrector high-throughput screening assays have relied on measurements of restored

Address correspondence to Raymond A Frizzell, University of Pittsburgh School of Medicine, Department of Cell Biology, Rangos Research Center, Room 7117, 4401 Penn Avenue, Pittsburgh, PA 15224. Phone: 412-692-9449; Fax: 412-692-8906; E-mail: frizzell@pitt.edu. Submitted January 3, 2012; Accepted for publication February 28, 2012; Epub (www.molmed.org) ahead of print February 29, 2012.

CFTR function. Halide sensitive yellow fluorescent proteins or Förster resonance energy transfer (FRET)-based voltage-sensitive membrane dyes have been used to detect plasma membrane F508del-CFTR function after small molecule treatment on the basis of detection of stimulated anion efflux from pre-loaded cells (13,14). Both of these methods require multiple wash steps and are susceptible to signal saturation. In addition, they rely on the recruitment of a functional CFTR to the cell surface. Alternatively, an immunofluorescence labeling method has been used with an epitope tagged version of CFTR to detect trafficking of mutant CFTR to the cell surface (20). This antibody-labeling approach also required multiple wash and binding steps, which add variability, reduce throughput for drug screening and can introduce artifacts due to cell permeabilization. Direct detection of F508del-CFTR at the cell surface with a single labeling step would improve throughput and increase the dynamic range of corrector screening assays.

Selective and sensitive detection of F508del-CFTR at the cell surface can be used to identify new correctors and can elucidate mechanisms for existing ones. However, this approach normally requires labor-intensive biochemical methods, such as immunofluorescence using epitope tags or biotinylation and subsequent immunoblotting techniques (21–23). To address these limitations, we tagged CFTR with a protein module that provides a unique and selective fluorescence assay of the abundance of this protein at the cell surface. The protein tag is comprised of a genetically encoded fluorogen-activating protein (FAP) that has been fused to the N-terminus or inserted in the fourth extracellular loop (EL4) of CFTR.

Here, we report the development of the FAP-CFTR platform and found the behavior as well as functional activity consistent with that of untagged WT and F508del-CFTR. Importantly, F508del-CFTR FAP constructs provide a method to quantify corrector efficacy that was

consistent with functional measurements of endogenous untagged CFTR in a native airway cell background. Using this method, we characterized two new correctors, Cystic Fibrosis Foundation Therapeutics (CFFT)-002 and C18, as well as corrector combinations that significantly improve the trafficking of F508del-CFTR compared with the previously described C4 corrector. Furthermore, this platform has a modular design to allow for rapid construction of FAP fusions with most transmembrane proteins. Therefore, this development can serve as a template for application to other protein trafficking diseases, to accelerate the discovery of pharmacological agents that rescue trafficking defects.

MATERIALS AND METHODS

Plasmids and Constructs

N-terminal fusions. FAP fusions to the N-terminus of CFTR with an additional membrane-spanning segment were generated using the pBabeSacLac2 plasmid, described previously (24). Briefly, CFTRs (both WT and F508del) were amplified by polymerase chain reaction (PCR) from pcDNA3 using primers that provided *SfiI* restriction sites (forward: GGCCCAGCCGGCCATGCAGAGGTCGCCTCTGGAA; reverse: GCCCCTGCGGCCCTA AAGCCTTGATCTTGCAC). First, a Malachite Green binding FAP (dNP138) was inserted into the Sac module of pBabeSacLac2 by *SfiI* digestion and ligation. Next, the CFTR PCR product was digested with *SfiI* and ligated into the Lac module via *PfmII-SfiI* hybrid sites. This step generated the plasmid pBabe dNP138-CFTR (WT or F508del).

EL4 fusions. Insertion of the FAP in the fourth extracellular loop of CFTR (both WT and F508del) was generated with a modified version of CFTR, where *KpnI* and *EcoRV* sites were introduced (a gift from Peter Haggie, University of California, San Francisco [UCSF]). The FAP (dNP138) was first amplified with *KpnI* and *EcoRV* containing primers then cut and inserted between the *KpnI* and *EcoRV* sites corresponding to the amino

acid sequence KGNSTHS(FAP)RNNSY. The sequence corresponding to CFTR ECL4-dNP138 was then transferred to a retroviral pBabe plasmid via *BamHI* and *XhoI* restriction sites for stable expression in mammalian cells.

Transduction

Transducing particles for pBabeSacLac2 constructs were generated using the Phoenix Ecotropic Packaging System (Nolan Laboratory, Stanford University, Stanford, CA, USA). Phoenix ecotropic cells (Phoenix-ECO) were plated at 1.3×10^6 cells/75-cm² flask in Dulbecco's modified Eagle's medium (DMEM) with calf serum without antibiotics. pBabeSacLac2 DNA was transfected as described above scaled to surface area. After 24 h, transfection complexes were removed and replaced with 8 mL DMEM with calf serum and incubated for 48 h at 32°C/5% CO₂. Medium was removed and filtered through a Millex-HV 0.45- μ m syringe filter and flash-frozen in liquid nitrogen. Recipient cells were plated at 2×10^5 cells/35-mm dish 24 h before transduction. Cells were infected by adding viral supernatant and 6 μ g/mL hexadimethrine bromide and incubated for 24 h at 32°C/5% CO₂. Cells were replated in 75-cm² flasks and screened for expression 48 h later.

Iodide Efflux Assay

CFTR/FAP fusion cell lines were assessed for CFTR anion transport activity by measuring the fluorescence of the halide-sensitive dye, 6-methoxy-N-(3-sulfopropyl) quinolinium (SPQ). Cells were plated on mattek dishes (part number p35G-1.5-14-C) 24 h before iodide efflux measurement, and correctors were added to the cells after 24 h and 24 h before iodide efflux measurements. A combination of 10 μ mol/L C4 + 5 μ mol/L C18, or dimethyl sulfoxide (DMSO) (vehicle), was added. SPQ was loaded into cells using a hypotonic iodide solution (above) that was diluted with H₂O 1:1 (v/v) and contained 10 mmol/L SPQ, and was incubated for 20 min at 37°C as previously described. After loading, cells

with SPQ were imaged at 40× on an inverted epi-fluorescence microscope equipped for excitation at 350 nm and emission at 455 nm; images were captured every 15 s. Cells were perfused with buffers warmed to 37°C. For each experiment, the following solutions were serially perfused across the cells: iodide buffer, 3 min; nitrate buffer, 3 min; nitrate buffer containing 10 μmol/L forskolin and a CFTR-specific potentiator, 300 nmol/L Potentiator-2 (P2) (obtained from Cystic Fibrosis Foundation Therapeutics), 6 or 8 min; and finally iodide buffer, 2 min. Analysis was performed with Image J by analyzing mean fluorescence intensity of preselected cells. Data are represented by the maximum slope of each iodide efflux for each condition measurement.

SPQ Solutions

Iodide solution contained 130 mmol/L NaI, 1 mmol/L Mg(NO₃)₂·6H₂O, Ca(NO₃)₂·4H₂O, 4 mmol/L KNO₃, 10 mmol/L glucose and 20 mmol/L N-2-hydroxyethylpiperazine-N'-2-ethanesulfonic acid (HEPES) hemisodium salt, pH 7.4. Nitrate solution contained 130 mmol/L NaNO₃, 1 mmol/L Mg(NO₃)₂·6H₂O, 1 mmol/L Ca(NO₃)₂·4H₂O, 4 mmol/L KNO₃, 10 mmol/L glucose and 20 mmol/L HEPES hemisodium salt, pH 7.4.

Flow Cytometry

Quantification of F508del-CFTR rescue to the cell surface was carried out by measurement of malachite green (MG)-11p fluorescence activity using flow cytometry. HEK293 cells stably expressing either FAP-F508del-CFTR or F508del-CFTR EL4-FAP were plated at a cell density of 1 × 10⁵ cells per 35-mm dish. After 12 h, the growth media were removed and replaced with 1 mL DMEM containing various corrector conditions: 10 μmol/L C4, 5 μmol/L CFFT-002, 5 μmol/L C18, 10 μmol/L C4 + 5 μmol/L CFFT-002, 10 μmol/L C4 + 5 μmol/L C18, 5 μmol/L CFFT-002 + 5 μmol/L C18 and vehicle (DMSO) (same volume as maximum used in corrector treatment). At 24 h after

corrector treatment, cells were removed from the dishes with Cellstripper™ (nonenzymatic, Cellgro), and cells were centrifuged at 500g for 5 min at 4°C and then resuspended in 1 mL PBS. MG-11p fluorogen (50 nmol/L) was added to all samples before measurement. Sample analysis was performed by excitation with a 640-nm laser, and emission was captured with a 685/35 filter set. Each condition consisted of 10,000 recorded events. Data analysis was performed using FACS Diva software to obtain the mean MG fluorescence ± standard error of the mean (SEM) for each population. The sample sizes for each condition were as follows: DMSO, C4 + C18 and CFFT-002 + C18, n = 5; C4, CFFT-002 and C18, n = 3. These represent experiments were performed on separate days. Each sample was normalized to the mean of C18.

Culture and Treatment of Human Bronchial Epithelial (HBE) Cells

Primary human bronchial epithelial (HBE) cells expressing F508del-CFTR cultured on 6.5-mm Transwell filters (Costar #3470) were obtained from the Human Airway Cell Core of the University of Pittsburgh Cystic Fibrosis Research Center. Cultures were differentiated until they developed beating cilia and electrical resistance >400 Ω/cm² (>3 wks). Cultures were treated with 5 μmol/L C18, 5 μmol/L CFFT-002 and a combination of the two by diluting a 1,000 × DMSO stock solution into fresh HBE culture medium. Treated cultures were incubated at 37°C for 18–24 h before Ussing chamber experiments.

HBE Culture

After proliferation, HBE cells were seeded on human placental collagen-coated Costar Transwell filters (catalog #3470; 0.33 cm², 0.4-μm pore) and maintained in a medium of 200 nmol/L Hydrocortisone (BD Biosciences #354203), 5 μg/mL insulin (Sigma #I9278), 10 μg/mL transferrin (BD Biosciences #354204), 3.3 μmol/L epinephrine (Sigma #E4250), 10 nmol/L triiodothyronine (Sigma #T6397), 0.5 ng/mL epidermal

growth factor (BD Biosciences #354001), 50 nmol/L retinoic acid (Sigma #R2625), 0.8% v/v bovine pituitary extract (Pel-Freez #57136-3), 0.5 μmol/L ethanolamine (Sigma #E9508), 0.5 μmol/L O-phosphorylethanolamine (Sigma #P0503), 0.5 mg/mL bovine serum albumin (Sigma #A3294), 0.5% v/v Ultrosor G (Crescent Chemical #12037-016), 1% stock 4 v/v (BioSource International #341-020), 0.1% v/v stock 11 (BioSource International #347-020), 1% v/v trace elements (BioSource International #349-100) and 1% cell culture PSF (Sigma #A5955) in 1 × DMEM/F12 (Invitrogen #11320-033).

Ussing Chamber Experiments

Filters were mounted in Ussing chambers (Physiologic Instruments #P2300). The basolateral bathing solution consisted of 120 mmol/L NaCl, 25 mmol/L NaHCO₃, 3.3 mmol/L KH₂PO₄, 0.8 mmol/L K₂HPO₄, 1.2 mmol/L CaCl₂, 1.2 mmol/L MgCl₂ and 10 mmol/L D-glucose. The apical bathing solution replaced 120 mmol/L NaCl with 120 mmol/L Na glutamate to achieve a transepithelial chloride gradient. The bathing solutions were gassed with 95% O₂ and 5% CO₂ to maintain a pH 7.4. Short-circuit current and transepithelial resistance were measured continuously using a voltage-clamp (VCC-MC8) and Acquire and Analyze v2.3 data acquisition hardware and software (Physiological Instruments, San Diego, CA, USA).

Filters were equilibrated for approximately 15 min to permit electrical parameters to stabilize, and then baseline short circuit current (I_{sc}) was measured. Amiloride (10 μmol/L) was added to the apical solution to inhibit epithelial sodium channel (ENaC)-mediated Na absorption. After 2 min, 20 μmol/L forskolin was added to the basolateral chamber to evoke CFTR-mediated anion secretion. After 3 min, 300 nmol/L CFTR P2 (<http://www.cftrfolding.org/CFTRReagents.htm>) was added to both solutions. After 2 min, 10 μmol/L CFTR inhibitor-172 was added to the apical solution. At these times, currents had achieved steady-state. Changes in short-

circuit currents were calculated from the mean currents obtained during the 10-s period preceding each drug addition.

Immunoblotting

Whole cell lysates from stably expressing FAP-tagged CFTR cell lines were obtained by removing cells from 10-cm dishes in radioimmunoprecipitation assay (RIPA) buffer: 150 mmol/L NaCl, 50 mmol/L Tris HCl, pH 7.5, 1% Triton \times 100, 1% sodium deoxycholate, 0.1% sodium dodecyl sulfate (SDS) and 1 tablet of protease inhibitor cocktail (PIC)/10 mL RIPA buffer (Roche #11-836-153-011). FAP-CFTR WT and CFTR WT EL4-FAP cell lines were grown under normal conditions; FAP-F508del-CFTR and F508del-CFTR EL4-FAP cell lines were treated with one of the following conditions for 24 h before harvesting whole cell lysates: (a) vehicle control (cell culture grade DMSO, at the volume used for correctors or corrector combinations); (b) CFFT-002 5 μ mol/L and C18 5 μ mol/L combination; or (c) C4 10 μ mol/L and C18 5 μ mol/L combination. Protein concentration was determined using a BCA protein assay, and 50 μ g protein was separated by sodium dodecyl sulfate–polyacrylamide gel electrophoresis (SDS-PAGE) using a 3% stacking gel and 5% resolving gel. Proteins were transferred to a polyvinylidene difluoride (PVDF) membrane (Immobilon-P PVDF membranes, Sigma-Aldrich, St. Louis, MO, USA) at 35 V for 18 h at 4°C. Membranes were blocked in 5% milk for 1 h at room temperature. Membranes were incubated overnight at 4°C and then 1 h at room temperature in Tris-buffered saline with Tween containing α CFTR#596 (<http://www.cftrfolding.org/CFFTReagents.htm>) at 1:5,000. Membranes were then incubated for 1 h at room temperature in donkey anti-mouse secondary (Jackson ImmunoResearch #715-005-150) at 1:10,000 and captured on film using a SuperSignal West Dura substrate kit (ThermoScientific #34076).

Microscope Image Acquisition

Images were acquired with NIS-Elements software using a Nikon Ti

eclipse confocal microscope with a Photometrics® Evolve™ EMCCD Camera camera by using 640-nm laser excitation and a 700/75-nm emission filter. The 40 \times (1.30 numerical aperture [NA]) and 60 \times (1.49 NA) objectives were used to image at room temperature with DMEM. Cells were plated on Mattek dishes (part number p35G-1.5-14-C). For F508del-expressing cell lines, cells were plated at a density of 1×10^5 cells. Cells were treated with C4 10 μ mol/L and C18 5 μ mol/L or vehicle (DMSO) control 12–24 h later. After 24 h of treatment, cells were imaged in the growth medium at 37°C and 5% CO₂ using confocal microscopy with either cell-impermeant (MG-11p) or cell-permeant (MG-Ester) dye at a concentration of 50 nmol/L. Low-temperature rescue was achieved by incubating cells at 30°C for 24 h. Fluorescence images of F508del-CFTR have scaled lookup tables that have been maintained across these experiments to increase contrast but are different from images acquired for CFTR WT using ImageJ software (National Institutes of Health (NIH), Bethesda, MD, USA; <http://rsbweb.nih.gov/ij/>). Therefore, comparison between CFTR WT and F508del images is not possible to estimate protein expression and abundance. The 10- μ m scale bars are indicated on each image.

Statistics

Statistical analysis was carried out using Graphpad Prism v5 software. A two-tailed unpaired Student *t* test was performed between each corrector condition and the DMSO vehicle-treated control. Statistical significance is represented as follows: **P* = 0.01–0.05; ***P* = 0.001–0.01, ****P* = 0.0001–0.001, *****P* < 0.0001.

Reagents

Corrector compounds C4, CFFT-002 and C18 were obtained from the CFFT panel library (www.cftrfolding.org). Cell-stripper was purchased from Mediatech (Manassas, VA, USA). Fluorogens, MG-11p and MG-ester were provided by the Molecular Biosensor and Imaging Center (MBIC) reagent chemistry group (Carnegie Mellon University).

All supplementary materials are available online at www.molmed.org.

RESULTS

Development of CFTR FAP Reporters and Their Labeling at the Cell Surface

The FAP system consists of a genetically encodable engineered antibody fragment (scFv) that binds a small organic dye called a “fluorogen.” The fluorogen is completely nonfluorescent in solution, but on binding to the FAP, its fluorescence activity is increased dramatically (15,000–20,000-fold) (25). The bipartite FAP and cognate fluorogen system enables the selective visualization of proteins at the cell surface through the use of a cell-impermeant fluorogen, MG, fused to an 11-unit polyethylene glycol linker (MG-11p). Alternatively, the total cellular distribution of FAP-tagged protein can be visualized using MG-ester, a fluorogen that passively diffuses across the cell membrane and is then trapped within the cell.

To use FAP-based detection for CFTR, we generated two separate CFTR tagging strategies, each of which presents the FAP tag to the extracellular environment, where it is accessible to the cell-impermeant fluorogen. First, we modified the N-terminus to include the FAP and an additional transmembrane segment, derived from the PDGF receptor; this is called FAP-CFTR (24). Second, we inserted the FAP tag into the fourth extracellular loop of CFTR, to generate CFTR EL4-FAP (Figure 1). EL4 is the largest extracellular domain in CFTR and has been used previously to insert epitope tags and fluorescent proteins (26–28). Because CFTR had been found to tolerate these modifications while retaining functional activity, we chose this location to create an FAP-CFTR chimeric protein. The CFTR EL4-FAP chimera was generated by inserting the FAP in the EL4 between the two asparagine residues required for the posttranslational glycosylation of CFTR (29,30).

To verify that the FAP reporter constructs behaved as expected, we expressed them in HEK293 cells and used

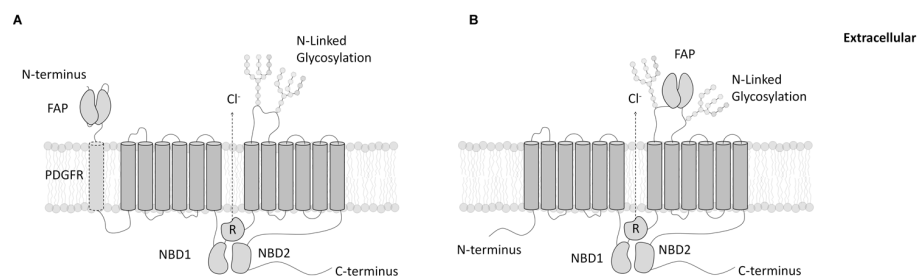


Figure 1. Topology of CFTR with FAP reporters. (A) Schematic diagram of CFTR tagged with a FAP reporter at the N-terminus via an extra transmembrane spanning fragment (FAP-CFTR). (B) Insertion of the FAP in the fourth extracellular loop of CFTR located between the two glycosylation sites (CFTR EL4-FAP).

the cell-impermeant fluorogen, MG-11p, to ask whether tagged WT CFTR had progressed to the cell surface. These cells were imaged using confocal fluorescence microscopy in the presence of either cell-impermeant or cell-permeant fluorogen, and representative images are provided in Figure 2. Distinct labeling of the cell membrane was observed with MG-11p (Figures 2A, C), which indicates that the CFTR WT FAP fusion proteins are trafficked to, and inserted in, the plasma membrane, exposing the FAP to the ex-

tracellular environment. When the same cells were exposed to MG-ester, there was a small, yet detectable, additional intracellular pool of protein, but the signal was predominantly localized to the cell surface (Figures 2B, D).

Visualization of F508del-CFTR Rescue

To study the trafficking defects of F508del-CFTR, we used FAP-CFTR and CFTR EL4-FAP constructs containing the F508del mutation to examine cellular location. HEK293 cells stably expressing ei-

ther the N-terminal or EL4 FAP F508del-CFTR constructs were grown under control conditions (vehicle, DMSO) for 24 h and imaged with MG-11p by confocal fluorescence microscopy. As expected, there was no signal because of the added fluorogen. The F508del-CFTR mutation prevented trafficking of the protein to the cell surface and presentation of FAP at the plasma membrane (Figures 3A, D). Consequently, the FAP is not exposed to the extracellular environment and is unable to bind and activate the cell-excluded MG-11p fluorogen. These images illustrate the low background level obtained from this technology, which can provide a large dynamic range for surface protein detection. To verify fusion protein expression under normal conditions, these cells were incubated with the cell-permeant fluorogen, MG-ester, which produced a significant intracellular expression pattern (Figures 3B, E). These observations are consistent with the trafficking defect of untagged F508del-CFTR, since the protein is translated and inserted into the endoplasmic reticulum membrane, but translocation to and beyond the Golgi is blocked.

Next, we tested whether the FAP fusions to F508del-CFTR were capable of pharmacological rescue by corrector compounds. Cells were treated with a combination of correctors (C4 and C18) for 24 h and then imaged with MG-11p fluorogen (Figures 3C, F). In contrast to the vehicle-treated control, both the N-terminal and the EL4 F508del-CFTR-expressing cell lines showed activation of the cell-impermeant fluorogen. This result demonstrated that the trafficking defect of F508del-CFTR had been rescued by corrector treatment and that the protein was present at the cell surface.

Low-temperature incubation ($\leq 30^{\circ}\text{C}$ for 24 h) is known to rescue the CFTR trafficking defect and allow some F508del-CFTR to accumulate at the cell surface. HEK293 cells expressing the F508del-CFTR FAP reporter constructs were incubated at low temperature and exposed to cell-impermeant fluorogen, and cell surface labeling was detected for

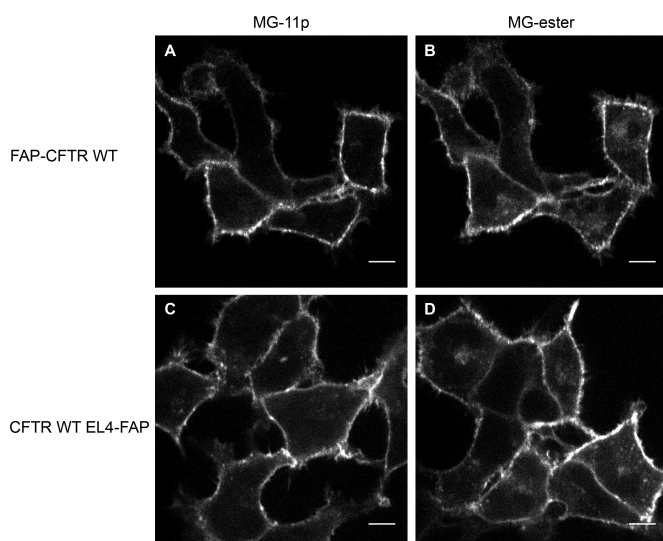


Figure 2. FAP detection of CFTR. HEK293 cells were imaged by confocal fluorescence microscopy. FAP-CFTR WT and CFTR WT EL4-FAP were detected exclusively at the cell surface using the cell-impermeant fluorogen MG-11p (A, C) or at the cell surface and in intracellular compartments throughout the cell with cell-permeant fluorogen MG-ester (B, D). The scale bars indicate 10 μm .

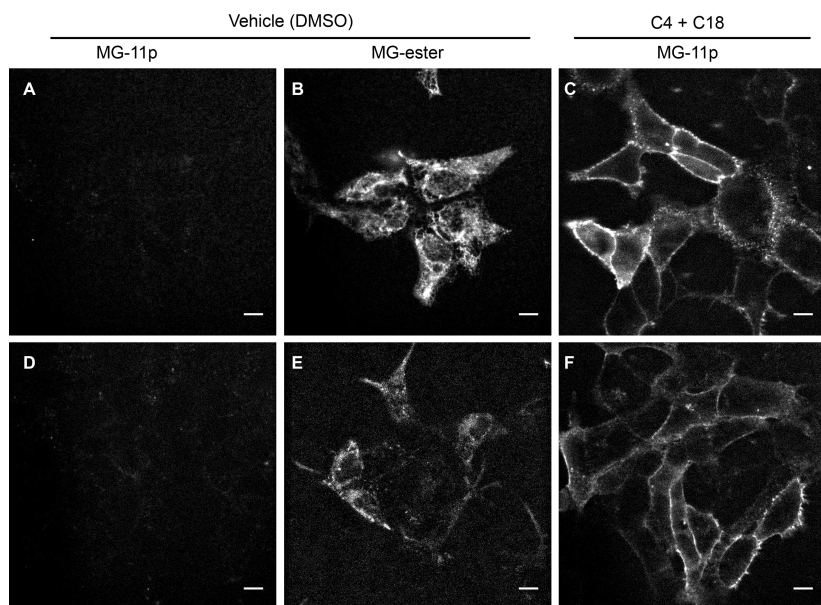


Figure 3. Correctors rescue the trafficking defect of FAP-CFTR F508del. HEK293 cells stably expressing FAP-F508del-CFTR (A–C) or F508del-CFTR EL4-FAP (D–F) were imaged using confocal fluorescence microscopy. After treatment with the vehicle (DMSO) control for 24 h, there was no staining observed in the presence of cell-impermeant fluorogen, 50 nmol/L MG-11p (A, D). A strong intracellular signal that was not localized to the plasma membrane was revealed on addition of the cell-permeant fluorogen, MG-ester (B, E). After treatment with a combination of correctors (C4 and C18 for 24 h), F508del-CFTR was detected at the cell surface using cell-impermeant fluorogen, 50 nmol/L MG-11p (C, F). The scale bars indicate 10 μ m.

cells incubated at the permissive temperature (30°C) (Figure 4).

Functional Rescue of F508del-CFTR

Next, we investigated whether the FAP reporter interfered with CFTR-mediated cAMP-stimulated anion transport by using a technique that measures regulated anion transport of anions across the plasma membrane using SPQ, a halide-sensitive fluorescent indicator dye. SPQ is quenched by iodide, so that the signal is weak in iodide-preloaded cells. Replacement of medium iodide with nitrate, which does not interact with SPQ, leads to dequenching of the signal in cells expressing functional CFTR at the plasma membrane upon treatment with forskolin. Using this approach, we found that both the HEK293 cells expressing the N-terminus or EL4 FAP tagged CFTR WT constructs displayed a characteristic pattern of CFTR-mediated iodide efflux

in response to forskolin stimulation (Figure 5A). Both the N-terminus and EL4 reporter constructs produced a rapid increase in SPQ fluorescence, which was consistent with that observed for untagged CFTR WT. Therefore, the cAMP-stimulated anion transport activity of CFTR is maintained with the FAP reporter modifications.

In the vehicle-treated controls, neither the N-terminal nor the EL4 FAP F508del-CFTR constructs significantly increased iodide efflux in response to stimulation (Figures 5B, C). To test whether the rescue of F508del-CFTR FAP trafficking results in the production of functional channels, we examined anion efflux in both cell lines after treatment with C4 and C18 correctors for 24 h. The corrector-treated cells generated substantial iodide efflux in response to stimulation that was completely absent in the vehicle-treated control groups (Figures 5B, C).

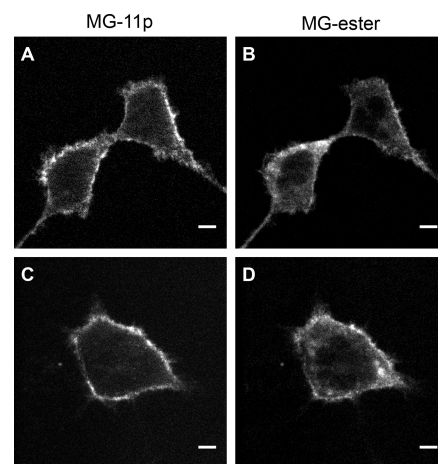


Figure 4. Temperature rescue of FAP-CFTR F508del. Rescue of FAP F508del-CFTR by low temperature visualized by confocal fluorescence microscopy is shown. HEK293 cells expressing FAP F508del-CFTR constructs were incubated at the permissive temperature (30°C) for 24 h. Surface expression was confirmed by activation of the impermeant fluorogen (50 nmol/L MG-11p) for both FAP-F508del-CFTR (A) and F508del-CFTR EL4-FAP (C). Cell-permeant staining with 50 nmol/L MG-ester revealed F508del-CFTR at both the cell surface and in intracellular pools (B), and a similar result was found for F508del-CFTR EL4-FAP (D). Controls without low temperature were as shown in Figures 3A and D. The scale bars indicate 10 μ m.

These results indicate that functional rescue of CFTR activity by corrector treatment, that is, anion transport across the plasma membrane, occurs with both of the FAP-tagged F508del-CFTR constructs.

Biochemical Rescue of F508del-CFTR

Next, F508del-CFTR FAP reporter protein expression was assessed by immunoblot analysis. The maturation of WT CFTR can be visualized as two bands on an SDS-PAGE gel: a more mobile core glycosylated form, having modifications acquired in the endoplasmic reticulum (B band), and a less mobile mature, complex glycosylated form, produced when the protein traverses the Golgi compartment (C band). Consistent with untagged WT

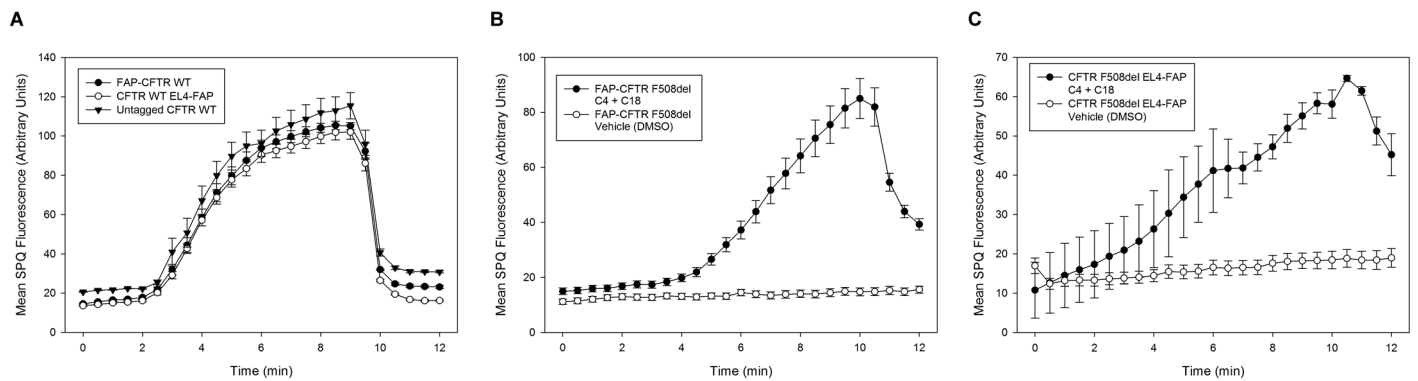


Figure 5. Correctors rescue F508del-CFTR FAP function. SPQ fluorescence traces showing iodide efflux in response to 10 $\mu\text{mol/L}$ forskolin stimulation are shown. (A) N-terminus and EL4 FAP-CFTR WT reporters show channel function overlapping with untagged CFTR WT. Stably expressing FAP-F508del-CFTR (B) or F508del-CFTR EL4-FAP (C) cells were treated with either vehicle (DMSO) or a combination of correctors (C4 + C18 for 24 h). Iodide efflux was stimulated with forskolin and a potentiator (300 nmol/L P2).

CFTR, FAP-CFTR WT migrated as two distinct bands, which we interpret as the core and mature (B and C, respectively) forms (Figure 6A), with increases in molecular weight attributed to the addition of the FAP tag (~ 20 kDa). On the other hand, CFTR WT EL4-FAP did not exhibit distinct B and C bands (see Figure 6A). Although a larger migrating band was present above the core glycosylated form, it did not show a discrete molecular weight shift expected from Golgi maturation.

Native F508del-CFTR does not produce a mature glycosylated band because it is retained in the endoplasmic reticulum and degraded before export to the Golgi. Previous studies have shown that correctors promote the maturation of F508del-CFTR, which can be visualized by the appearance of band C (13,14). To test whether the F508del-CFTR FAP reporter proteins also exhibit this behavior, we performed immunoblots using the CFTR-specific antibody, CFFT#596. Whole cell lysates from stable HEK293 cell lines expressing either the FAP-F508del-CFTR or the F508del-CFTR EL4-FAP were extracted from cells that had been treated with correctors or vehicle (DMSO). FAP-F508del-CFTR acquired a band that migrated at the same position as the C band of FAP-CFTR WT after corrector

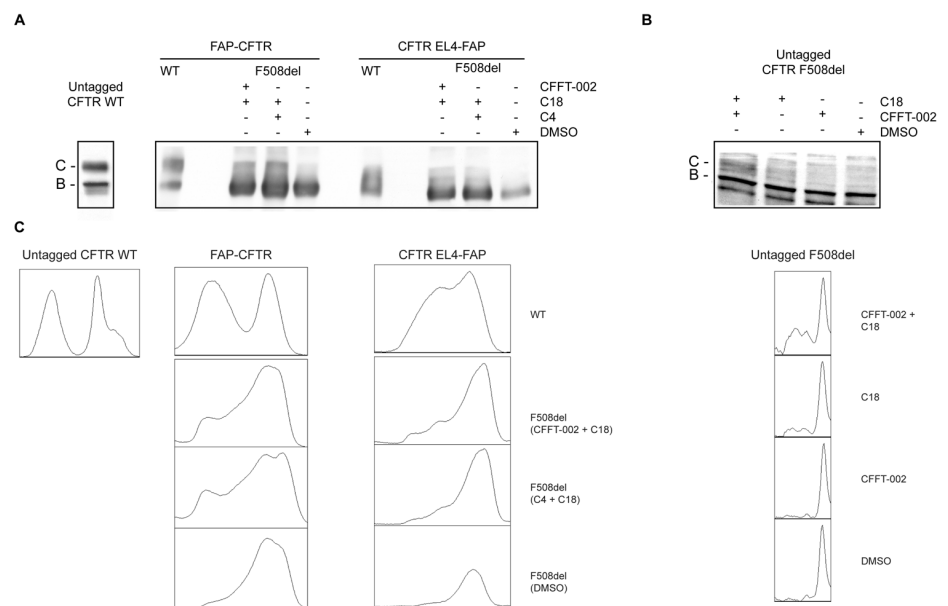


Figure 6. Biochemical properties of FAP-CFTRs and evidence of corrector rescue. Immunoblots were performed on whole cell lysates from cells expressing CFTR. (A) HEK293 cells expressing either untagged or FAP-CFTR constructs. F508del constructs receiving treatment with correctors CFFT-002 + C18 or C4 + C18 for 24 h showed an accumulation of higher-molecular weight bands that were not present in the vehicle-treated control. FAP-F508del-CFTR corrected lanes have acquired a fully glycosylated C band, but corrected F508del-CFTR EL4-FAP shows incomplete glycosylation. (B) HBE cells expressing untagged F508del were treated with CFFT-002 and C18 either alone or in combination. Mature glycosylated bands were detected with a combination of corrector treatments but not under control conditions. These biochemical findings agree with the results from cell surface labeling and function (Figure 7D, Table 1). (C) Densitometry analysis of these immunoblots shows decreasing molecular weight from left to right. Clear differences are observed between the combination of corrector treatment and vehicle.

treatment with either the CFFT-002 + C18 or C4 + C18 combinations. This pattern was not evident in the vehicle control lysates (see Figure 6A). Like FAP-CFTR WT, F508del-CFTR EL4-FAP acquired higher molecular weight bands after both corrector treatments (CFFT-002 + C18), which were absent under control conditions (see Figure 6A). Complete glycosylation was not achieved for the F508del-CFTR EL4-FAP relative to the N-terminal FAP tag, even after corrector treatment, an observation that is consistent also for CFTR WT EL4-FAP. In HBE cells, which express endogenous untagged CFTR F508del, rescue of a mature glycosylated band was detected after treatment with a combination of CFFT-002 and C18, and at a lower density after treatment with C18 alone, and was not evident under control conditions or after CFFT-002 (Figure 6B). Densitometry plots of each of the lanes from these immunoblots were generated to facilitate detection and interpretation of antibody labeling (Figure 6C).

Quantification of Corrector Efficacy

To gain insight on their individual properties and to characterize available correctors and combinations, we used flow cytometry to accurately quantify the effects of each corrector condition on the rescue of cell surface CFTR. Flow cytometry offers a quantitative output of the fluorescence of each cell, while also providing information on the distribution of fluorescence across a large cell population. We analyzed 10,000 cells per condition and took the average fluorescence intensity from activation of the MG-11p signal, which reduced the effects of heterogeneity between cells due to expression differences and other factors such as cell cycle. HEK293 cell lines expressing either FAP-F508del-CFTR or F508del-CFTR EL4-FAP were incubated with single correctors or combinations of correctors at their maximal effective concentrations for 24 h. After corrector treatment, the cells were brought into suspension using a nonenzymatic reagent to ensure that proteins at the cell surface remained intact,

Table 1. Summary of corrector efficacy from FAP labeling and functional assays.

	FAP-F508del-CFTR	F508del-CFTR EL4-FAP	HBE F508del-CFTR
DMSO	0.34	0.37	0.18
C4	0.53	0.51	0.25
CFFT-002	0.55	0.48	0.5
C18	1	1	1
C4 + CFFT-002	0.68	0.52	0.58
C4 + C18	2.11	1.29	0.96
C18 + CFFT-002	1.97	1.37	1.3

The corrector efficacy for single compounds and combinations summarized from Figures 7B, C and D is shown. Results are mean value normalized to C18.

an issue that complicates enzymatic procedures such as trypsinization. Samples were analyzed in the presence of cell-impermeant fluorogen, MG-11p, and the fluorescence activation across the population over three independent trials was normalized to the signal obtained for C18 (see Table 1 for a summary of corrector efficacy data). A representative output of these experiments is shown in Figure 7A. C18 + CFFT-002 treatment produced a dramatic increase in signal in the FAP-F508del-CFTR samples and a lesser increase in the F508del-CFTR EL4-FAP samples.

The well-studied corrector C4 produced a small improvement in plasma membrane density compared with the vehicle-treated control (0.53 versus 0.34 and 0.51 versus 0.37 for both the N-terminus and EL4 F508del-CFTR constructs, respectively) (Figures 7B, C). A statistically significant difference was found for FAP-F508del-CFTR when treated with C4 but not for F508del-CFTR EL4-FAP. Another corrector, CFFT-002, performed similarly to C4, increasing the density of the N-terminus and EL4 fusions at the cell surface to 0.55 and 0.47, respectively (see Figures 7B, C). The most potent single agent corrector tested was C18. Levels of trafficking correction reached 3.5-fold better than observed for the reference corrector, C4, for the N-terminus tagged F508del-CFTR construct after subtraction of the vehicle (DMSO) control.

Combinations of correctors were tested to assess whether they produced more robust rescue when used together. In the

FAP-F508del-CFTR-expressing cells, a combination of C4 and CFFT-002 did not statistically improve the efficacy over either compound alone (see Figure 7B). A combination of CFFT-002 and C18, however, resulted in a significant increase in surface expression, resulting in an 8.6-fold increase over the rescue achieved by C4 alone. Similarly, C4 and C18 treatment produced a 9.3-fold improvement compared with C4 correction. There was no statistically significant difference found for the CFFT-002 + C18 versus C4 + C18 corrector conditions. Even though all of the correctors were used at their maximal effective concentrations, the FAP-F508del-CFTR construct showed greatly improved trafficking with the corrector combinations C4 + C18 or CFFT-002 + C18 compared with single-compound treatments (Table 1 and Figure 7B).

The F508del-CFTR EL4-FAP-expressing cell line similarly did not show a robust increase of surface expression for the C4 and CFFT-002 corrector combination compared with either compound alone. Combinations of corrector treatments increased the relative plasma membrane density from 0.51 with C4 alone to 1.29 and 1.37 with C4 + C18 or C18 + CFFT-002, respectively (Table 1 and Figure 7C). No statistical difference was observed between the corrector combinations CFFT-002 + C18 and C4 + C18. Both corrector combinations increased the plasma membrane density of F508del-CFTR EL4-FAP over the single corrector treatments alone; however, the level of improvement was not as robust as the effect seen

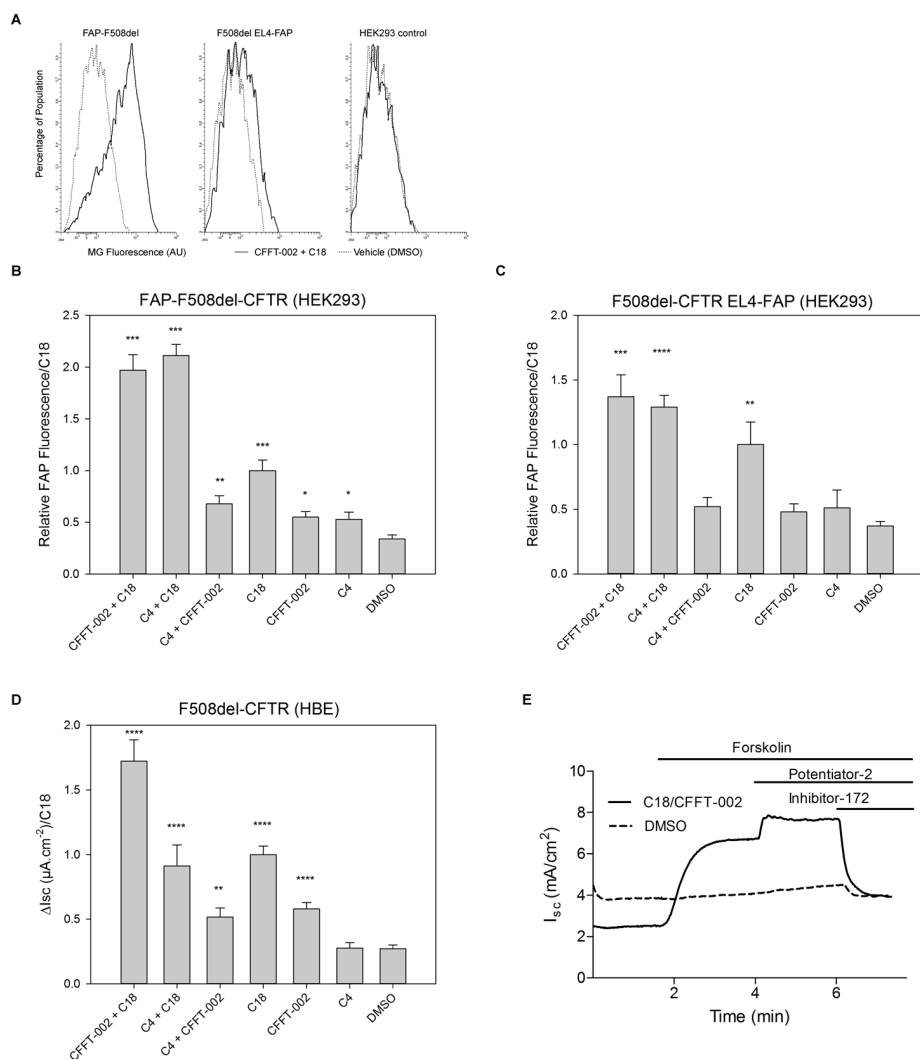


Figure 7. Quantification of corrector efficacy by flow cytometry and short circuit current measurements. Corrector efficacies of single-corrector compounds or combinations, determined by flow cytometry or Ussing chamber measurements are shown. (A) A representative flow cytometry histogram for HEK293 cell lines showing the distribution of MG-11p fluorescence signal for the vehicle control (dashed line) and CFFT-002 + C18 (solid line) corrector treatment. Fluorescence activity is plotted along the horizontal axis using a logarithmic scale. Bar graphs show the mean fluorescence intensity of HEK293 cells expressing either FAP-F508del-CFTR (B) or F508del-CFTR EL4-FAP (C) for each condition, normalized to the effect of C18. Data are presented as the mean \pm SEM ($n = 3$). (D) Short circuit currents were measured across polarized HBE cells, which express endogenous, untagged F508del-CFTR. Corrector efficacy was determined from the currents generated by addition of forskolin and potentiator P2, as described in Research Design and Methods and normalized to the current obtained for C18-treated epithelia ($9.0 \pm 1.1 \Delta I_{sc}$ ($\mu A/cm^2$)). Data are presented as the mean \pm SEM ($n = 6$ and $n = 36$ total observations). (E) Representative traces of short-circuit current (I_{sc}) across primary cultures of HBE cells mounted in Ussing chambers. I_{sc} was measured after treatment of HBE cells with the corrector combination, C18 + CFFT-002, or vehicle (DMSO) for 24 h. Statistical significance is represented as follows: * $P = 0.01$ – 0.05 ; ** $P = 0.001$ – 0.01 , *** $P = 0.0001$ – 0.001 , **** $P < 0.0001$.

from the FAP-F508del-CFTR cell line (Table 1 and Figure 7C).

Corrector Efficacy in F508del-CFTR-Expressing HBE Cells

HBE cells have emerged as a validated preclinical system in drug discovery for CF (31). Efficacy data obtained from anion transport measurements in differentiated HBE cells, together with acceptable toxicology outcomes, can advance candidate small molecules to clinical trials. Therefore, this system can provide a reference for evaluating the potential of the FAP approach as a screen for drug discovery or development. We cultured HBE cells from CF patients homozygous for the F508del mutation to compare the rescue of stimulated anion transport, measured as a transepithelial current in Ussing chambers, with the data obtained from the HEK293 FAP-tagged F508del-CFTR cell lines. In these studies, C4 showed no statistically significant rescue of F508del-CFTR currents over vehicle-treated controls. Consistent with data obtained in HEK293 cells, however, we found that the most potent single compound in primary HBE cells was C18, which significantly rescued channel function compared with control-treated cells (Figure 7D). The combination of CFFT-002 and C18, but not C4 and the other correctors, increased the extent of functional rescue compared with these compounds when used individually. Figure 7E shows a representative trace from these Ussing chamber experiments with the most robust combination of correctors, C18 + CFFT-002. Although some quantitative differences emerge from the comparison of HEK293 and HBE cells, the data were qualitatively similar in these very different systems and assays.

DISCUSSION

Selective detection of proteins at the cell surface is a prerequisite for studying the trafficking behavior of membrane proteins, such as CFTR, to and from the plasma membrane and for evaluating therapeutic approaches to diseases of protein folding. Traditionally, this has

been accomplished by time- and labor-intensive biochemical labeling methods such as biotinylation and immunofluorescence. By using a genetically encoded FAP reporter, however, we can selectively label CFTR at the cell surface in live cells instantly without the need for incubation or wash steps that may modify the cellular handling of CFTR. The cell-impermeant fluorogen remains dark when free in solution; however, upon binding to the FAP, fluorogen fluorescence increases >15,000-fold. These features provide low background signal, excellent signal-to-noise and a large dynamic range, and they eliminate the need for wash or blocking steps to remove nonspecific signals. Proper trafficking and localization of FAP-tagged CFTR to the cell surface was confirmed using confocal fluorescence microscopy in stable cell lines. Importantly, F508del-CFTR FAP protein was absent from the plasma membrane under normal conditions, but was readily detected by cell-impermeant fluorogen after treatment by currently available correctors.

Immunoblot analysis was used to reveal the glycosylation state of the FAP-CFTR WT and CFTR WT EL4-FAP fusion constructs. The N-terminal FAP-CFTR WT fusion protein migrated as two distinct bands, the core and mature bands characteristic of untagged CFTR WT. The CFTR EL4-FAP construct did not produce a distinct mature band, which suggests that the efficiency of its glycosylation was impaired. The fourth extracellular loop of CFTR is the locus of two asparagine residues (N894 and N900) that acquire N-linked glycosylation and other modifications; therefore, careful consideration was taken to preserve these residues, and the consensus glycosylation sequences (NXS/T) surrounding them, in the FAP fusion construct (29,30). The observed incomplete glycosylation could be due to reduced glycan modification or partial oligosaccharide modification at these sites, which may result from impaired glycosylation enzyme recognition and/or accessibility at these sites when the FAP tag is pres-

ent. Modification of the FAP location within EL4 or by varying the spacer length and/or properties may improve glycosylation. However, in view of the adequacy of the N-terminal reporter, this step has not been pursued.

Importantly, immunoblots showed that corrector treatment was capable of rescuing the maturation of FAP-F508del-CFTR, albeit modestly (Figure 6). Accumulation of the C band after corrector treatment is quite low with untagged F508del-CFTR and can depend on the cell type examined (13,15). To date, C4 is one of the most well-studied correctors for F508del-CFTR rescue. However, the efficiency of rescue for C4 is quite limited across multiple cell types that have been tested (15,18,32). This result is in agreement with data obtained from both F508del-CFTR FAP constructs in HEK293 cells as well as the currents associated with F508del-CFTR endogenously expressed from HBE cells, where functional C4 correction efficacy was poor (Table 1). Unlike C4, C18 displayed a more robust rescue in both HEK293 cells expressing FAP-CFTR constructs and in HBE cells expressing endogenous F508del-CFTR. Because rescue by C18 was independent of cellular background, this molecule may interact directly with F508del-CFTR or through a common quality control pathway expressed in both systems. Future studies to determine the exact mechanism of these correctors, especially C18 and related compounds, will increase our understanding of the F508del-CFTR folding defect and can help guide the design of new and more effective correctors or corrector combinations.

Combinations of corrector treatments, particularly CFFT-002 and C18, improved F508del-CFTR trafficking and function over single corrector treatments alone (Table 1). The enhanced effects produced from combinations of correctors, acting at their maximally effective concentrations, indicate that these corrector compounds likely have distinct targets and/or mechanisms of action. One possibility is that each corrector interacts with a different structural feature of F508del-CFTR to sta-

bilize their folding or reduce nonproductive folding intermediates. Because the folding defect of F508del involves multiple domain and interdomain interactions, multiple interaction sites may be necessary for optimal correction of the misfolded protein (33–37). Alternatively, rescue might be achieved indirectly through the modulation of folding chaperones or by suppressing ER-associated degradation (ERAD) quality control pathways that promote F508del-CFTR ubiquitylation and degradation. In addition, since rescued F508del-CFTR may also be subject to quality control pathways at the cell surface, rescue improvements may arise via actions at different cell loci (28,38). Because the development of combination therapies to correct CFTR trafficking may be required to obtain sufficient efficacy, the availability of a method with a broad dynamic range should optimize the detection of a signal that approaches that of WT CFTR.

Alternative tagging strategies were used to study CFTR to minimize artifacts due to the fluorescent reporter position. Although, the N-terminus and EL4 constructs both produced functional CFTR fusion proteins for which behavior was qualitatively similar, there were some important differences between them. In addition to the impaired glycosylation of the EL4 constructs, the plasma membrane density and anion transport of F508del-CFTR EL4-FAP, even after corrector treatment, was substantially diminished compared with the N-terminal fusion. Therefore, the N-terminal fusion appears to be superior because of its more robust expression, glycosylation state and anion transport capabilities.

The pattern of corrector efficacy was strikingly similar across the disparate cell types and assays that we examined, and this has not always been observed (15,16). Nevertheless, our results highlight the fidelity of the FAP reporter system to recapitulate the behavior of F508del-CFTR in a system that expresses the mutant untagged protein endogenously. Taken together, these re-

sults demonstrate that the FAP reporter system is sensitive enough to elucidate differences in the extent of correction of cell surface expression among different correctors. Moreover, this pattern of corrector action correlates with functional data obtained from differentiated human airway epithelia, a drug development system that has enabled the transition from preclinical data to clinical trials (39,40).

CONCLUSION

The development of this unique fluorescent detection platform addresses a largely unmet need in CF research, providing the ability to rapidly detect CFTR at the cell surface. Considerable progress has been made toward understanding the biology and physiology of CFTR; however, technological restrictions such as limited dynamic range, multiple wash and labeling steps and long data acquisition times may have hampered drug development. As a proof of principle, this system has been validated with known corrector compounds, but could be adapted to a multi-well format to screen for new correctors. Therefore, this fluorescence-based approach could streamline the current drug development pipeline. Moreover, this system was designed in a manner that could make it generally adaptable to other conditions that impair protein folding and/or plasma membrane trafficking. This growing list includes diseases such as type 2 diabetes (glucose transporter [GLUT]-4, insulin receptor), long QT syndrome (hERG), familial hypercholesterolemia (low-density lipoprotein [LDL] receptor), diabetes insipidus (aquaporin-2), diseases of retinal degeneration (bestrophin-1 [BEST1]) and others.

ACKNOWLEDGMENTS

The authors thank Martin Mense (Cystic Fibrosis Foundation Therapeutics) for providing CFFT-002 and Peter Haggie (UCSF) for the CFTR-EL4 plasmid. This work was supported by the National Center for Research Resources, NIH (grant U54 RR022241); NIH grants P30

DK072506 and DK68196; and a grant from the Cystic Fibrosis Foundation (FRIZZE05XX0).

DISCLOSURE

JW Jarvik is a founder and shareholder in SpectraGenetics Inc., a company that has expressed interest in licensing rights to FAP-tagged CFTR from Carnegie Mellon University.

REFERENCES

- Riordan JR, et al. (1989) Identification of the cystic fibrosis gene: cloning and characterization of complementary DNA. *Science*. 245:1066–73.
- Rommens JM, et al. (1989) Identification of the cystic fibrosis gene: chromosome walking and jumping. *Science*. 245:1059–65.
- Sheppard DN, Welsh MJ. (1999) Structure and function of the CFTR chloride channel. *Physiol. Rev.* 79 (Suppl. 1):S23–45.
- Bobadilla JL, et al. (2002) Cystic fibrosis: a worldwide analysis of CFTR mutations: correlation with incidence data and application to screening. *Hum. Mutat.* 19:575–606.
- Welsh MJ, et al. (1993) Dysfunction of CFTR bearing the delta F508 mutation. *J. Cell Sci. Suppl.* 17:235–9.
- Denning GM, et al. (1992) Processing of mutant cystic fibrosis transmembrane conductance regulator is temperature-sensitive. *Nature*. 358:761–4.
- Sato S, et al. (1996) Glycerol reverses the misfolding phenotype of the most common cystic fibrosis mutation. *J. Biol. Chem.* 271:635–8.
- Brown CR, et al. (1996) Chemical chaperones correct the mutant phenotype of the delta F508 cystic fibrosis transmembrane conductance regulator protein. *Cell Stress Chaperones*. 1:117–25.
- Galiotta LJ, et al. (2001) Novel CFTR chloride channel activators identified by screening of combinatorial libraries based on flavone and benzoquinolinizinium lead compounds. *J. Biol. Chem.* 276:19723–8.
- Pedemonte N, et al. (2005) Phenylglycine and sulfonamide correctors of defective delta F508 and G551D cystic fibrosis transmembrane conductance regulator chloride-channel gating. *Mol. Pharmacol.* 67:1797–807.
- Van Goor F, et al. (2009) Rescue of CF airway epithelial cell function in vitro by a CFTR potentiator, VX-770. *Proc. Natl. Acad. Sci. U. S. A.* 106:18825–30.
- Yang H, et al. (2003) Nanomolar affinity small molecule correctors of defective delta F508-CFTR chloride channel gating. *J. Biol. Chem.* 278:35079–85.
- Pedemonte N, et al. (2005) Small-molecule correctors of defective deltaF508-CFTR cellular processing identified by high-throughput screening. *J. Clin. Invest.* 115:2564–71.
- Van Goor F, et al. (2006) Rescue of deltaF508-CFTR trafficking and gating in human cystic fibrosis airway primary cultures by small molecules. *Am. J. Physiol. Lung Cell. Mol. Physiol.* 290:L1117–30.
- Pedemonte N, et al. (2010) Influence of cell background on pharmacological rescue of mutant CFTR. *Am. J. Physiol. Cell Physiol.* 298:C866–74.
- Sondo E, et al. (2011) Rescue of the mutant CFTR chloride channel by pharmacological correctors and low temperature analyzed by gene expression profiling. *Am. J. Physiol. Cell Physiol.* 301:C872–85.
- Lin S, et al. (2010) Identification of synergistic combinations of F508del cystic fibrosis transmembrane conductance regulator (CFTR) modulators. *Assay Drug Dev. Technol.* 8:669–84.
- Cholon DM, et al. (2010) Modulation of endocytic trafficking and apical stability of CFTR in primary human airway epithelial cultures. *Am. J. Physiol. Lung Cell. Mol. Physiol.* 298:L304–14.
- Wang Y, et al. (2007) Additive effect of multiple pharmacological chaperones on maturation of CFTR processing mutants. *Biochem. J.* 406:257–63.
- Carlile GW, et al. (2007) Correctors of protein trafficking defects identified by a novel high-throughput screening assay. *Chembiochem*. 8:1012–20.
- Okiyonedo T, et al. (2010) Peripheral protein quality control removes unfolded CFTR from the plasma membrane. *Science*. 329:805–10.
- Luo Y, McDonald K, Hanrahan JW. (2009) Trafficking of immature deltaF508-CFTR to the plasma membrane and its detection by biotinylation. *Biochem. J.* 419:211–9.
- Gentzsch M, et al. (2004) Endocytic trafficking routes of wild type and deltaF508 cystic fibrosis transmembrane conductance regulator. *Mol. Biol. Cell.* 15:2684–96.
- Holleran J, et al. (2010) Fluorogen-activating proteins as biosensors of cell-surface proteins in living cells. *Cytometry A.* 77:776–82.
- Szent-Gyorgyi C, et al. (2008) Fluorogen-activating single-chain antibodies for imaging cell surface proteins. *Nature Biotechnol.* 26:235–40.
- Haggie PM, Verkman AS. (2008) Monomeric CFTR in plasma membranes in live cells revealed by single molecule fluorescence imaging. *J. Biol. Chem.* 283:23510–3.
- Howard M, et al. (1995) Epitope tagging permits cell surface detection of functional CFTR. *Am. J. Physiol.* 269:C1565–76.
- Sharma M, et al. (2004) Misfolding diverts CFTR from recycling to degradation: quality control at early endosomes. *J. Cell Biol.* 164:923–33.
- Glozman R, et al. (2009) N-glycans are direct determinants of CFTR folding and stability in secretory and endocytic membrane traffic. *J. Cell Biol.* 184:847–62.
- Chang XB, et al. (2008) Role of N-linked oligosaccharides in the biosynthetic processing of the cystic fibrosis membrane conductance regulator. *J. Cell Sci.* 121:2814–23.
- Van Goor F, et al. (2011) Correction of the F508del-CFTR protein processing defect in vitro by the investigational drug VX-809. *Proc. Natl. Acad. Sci. U. S. A.* 108:18843–8.

32. Varga K, *et al.* (2008) Enhanced cell-surface stability of rescued deltaF508 cystic fibrosis transmembrane conductance regulator (CFTR) by pharmacological chaperones. *Biochem. J.* 410:555–64.
33. Mornon JP, Lehn P, Callebaut I. (2008) Atomic model of human cystic fibrosis transmembrane conductance regulator: membrane-spanning domains and coupling interfaces. *Cell. Mol. Life Sci.* 65:2594–612.
34. Mornon JP, Lehn P, Callebaut I. (2009) Molecular models of the open and closed states of the whole human CFTR protein. *Cell Mol. Life Sci.* 66:3469–86.
35. Serohijos AW, *et al.* (2008) Phenylalanine-508 mediates a cytoplasmic-membrane domain contact in the CFTR 3D structure crucial to assembly and channel function. *Proc. Natl. Acad. Sci. U. S. A.* 105:3256–61.
36. Rabeh WM, *et al.* (2012) Correction of both NBD1 energetics and domain interface is required to restore deltaF508 CFTR folding and function. *Cell.* 148:150–63.
37. Mendoza JL, *et al.* (2012) Requirements for efficient correction of deltaF508 CFTR revealed by analyses of evolved sequences. *Cell.* 148:164–74.
38. Okiyoneda T, Apaja PM, Lukacs GL. (2011) Protein quality control at the plasma membrane. *Curr. Opin. Cell Biol.* 23:483–91.
39. Accurso FJ, *et al.* (2010) Effect of VX-770 in persons with cystic fibrosis and the G551D-CFTR mutation. *N. Engl. J. Med.* 363:1991–2003.
40. Clancy JP, *et al.* (2012) Results of a phase IIa study of VX-809, an investigational CFTR corrector compound, in subjects with cystic fibrosis homozygous for the F508del-CFTR mutation. *Thorax.* 67:12–8.